KLOE note n. 143
April 1995

Ageing test of the KLOE Drift Chamber Wires

G. Bencivenni, L. Bucci, R. de Sangro, G. Finocchiaro, P. Valente

INFN, Laboratori Nazionali di Frascati

ABSTRACT

We present the results of tests of accelerated ageing, performed to check the capability of the KLOE drift chamber wires to withstand the (not severe) radiation doses during its operation at DAΦNE. The results indicate that the wire ageing is negligible for all the wire-cell configurations tested.

1. Introduction

In the KLOE drift chamber we will have approximately $3\,\mathrm{m}\times 40{,}000 \simeq 120\,\mathrm{km}$ of field wires. The purpose of the work described in this note is to test the ageing properties of the combination gas/wires/cell that we will be using in the KLOE drift chamber.

1.1 Radiation estimates for KLOE

Radiation damage on the wires of the drift chamber can be due either to "machine related" effects, or to "physics" processes. Touscheck effect is dominant over other beam related backgrounds, such as Coulomb scattering and bremsstrahlung in the residual gas in the DAΦNE vacuum chamber [1,2].

At the maximum DAΦNE current and number of bunches, and assuming the largest proposed dimensions for the beam scrapers, the rate of 'Touscheck' electrons impinging onto the beam pipe at the KLOE interaction region is $\simeq 6.4\cdot 10^5$ Hz [1]. Making the very pessimistic assumption that *all* these electrons reach the chamber, their rate on 1 cm of wire belonging to the innermost layer (located at $R \simeq 30$ cm from the centre in the $R-\phi$ plane) is $\simeq 25$ Hz, assuming a flat distribution in z and φ. However, one should consider that these electrons could also initiate showers on the beam pipe and in the low β quadrupoles, an effect which could be more realistically estimated with a detailed simulation.

Small angle Bhabha electrons (or positrons) hitting the corners of the quadrupoles are in principle even more dangerous in this respect, since the cross section is larger and the source is localised. Their effect has been simulated in [3] to study the trigger rate in the endcaps of the e.m. calorimeter. From the numbers quoted in this note, we estimate (1) that the contribution of this effect to the wire ageing is negligible compared to the one due to 'true' Bhabha scattering, which is by far the most abundant physics process, especially at small polar angles.

The charge collected during a given running period on a segment of wire L_{w} cm long as a consequence of the incident Bhabha radiation is

$$Q = Q_{\mathrm{e}} \cdot A_{\mathrm{gas}} \cdot \langle N_{\mathrm{cl}} \cdot N^e \rangle_{\mathrm{MIP}} \cdot K_{\mathrm{r.r.}} \cdot L_{\mathrm{w}} \cdot \sigma_{\mathrm{cell}}(\vartheta) \cdot \int \mathcal{L}\mathrm{dt}.$$

Here $Q_{\mathrm{e}} = 1.6 \cdot 10^{-19}$ C is the electron charge, A_{gas} is the gas amplification, $\langle N_{\mathrm{cl}} \cdot N^e \rangle_{\mathrm{MIP}}$ the mean number of clusters released per cm of gas by a minimum ionising particle, times their average electron multiplicity. In the 90%He$-$10%$i\mathrm{C_4H_{10}}$ gas mixture which we intend to use in the KLOE drift chamber and which was used in the present tests, $A_{\mathrm{gas}} \simeq 10^5$, $\langle N_{\mathrm{cl}} \cdot N^e \rangle_{\mathrm{MIP}} \simeq 13 \cdot 1.66\,\mathrm{cm}^{-1}$ [4,5]. $K_{\mathrm{r.r.}}$ accounts for the relativistic rise in the energy loss expected for relativistic Bhabha electrons ($K_{\mathrm{r.r.}} \simeq 1.3$ in 90%He$-$10%$i\mathrm{C_4H_{10}}$).

We define as $\sigma_{\mathrm{cell}}(\vartheta) \equiv \sigma(\vartheta) \times w_{\mathrm{cell}}/(2\pi R)$ the Bhabha cross section in one single cell of width w_{cell} at a radial distance R from the centre.

Assuming $L_{\mathrm{w}} = 1\,\mathrm{cm}$ and $w_{\mathrm{cell}} = 2\,\mathrm{cm}$, the charge integrated in 1 year ($\equiv 10^7$ sec) of running time at a luminosity $\mathcal{L} = 5 \times 10^{32}\,\mathrm{s}^{-1}\,\mathrm{cm}^{-2}$ is

$$Q_{1\,\mathrm{year}}(\mu\mathrm{C/cm}) = 714 \times \frac{\sigma(\mu\mathrm{b})}{R(\mathrm{cm})}.$$

Given the geometry of the drift chamber, the zone receiving the largest dose of Bhabha electrons is located at $|z| = 142\,\mathrm{cm}$, $R = 29.5\,\mathrm{cm}$. The Bhabha cross section for $28.5\,\mathrm{cm} \leqslant R \leqslant 30.5\,\mathrm{cm}$, *i.e.* $11.4^\circ \leqslant \vartheta \leqslant 12.1^\circ$ (remember that we are dealing with 2×2 square cells), integrated over the whole azimuthal angle, is $3.16\,\mu\mathrm{b}$, hence $\simeq 45\,\mathrm{Hz}$ in one cell at $R = 29.5\,\mathrm{cm}$. Plugging the numbers in the formula above, one gets $Q_{1\,\mathrm{year}} = 76\mu\mathrm{C/cm}$ in the worst possible case.

(1) The largest quadrupole has a maximum radius of 13.5 cm. Due to the KLOE magnetic field of 6 kG, a charged particle generated at the quadrupole must therefore have a minimum transverse momentum of $p_\perp^{\mathrm{min}} = 15\,\mathrm{MeV}/c$, in order to reach $R = 30\,\mathrm{cm}$. Interpolating from the first table at page 4 in [3], the total rate of particles (e^+e^- and γ's) releasing in one endcap more than 15 MeV *energy* is 344 kHz. Out of these only $\lesssim 5\%$ are charged (fig. 5, *ibidem*), $\simeq 10\%$ have $\mathrm{p} \geq 15\,\mathrm{MeV}/c$ (fig. 6 *ibidem*), and $\simeq 1/60$ are in the azimuthal range of 1 cell at $R = 30\,\mathrm{cm}$, bringing down the rate to 30 Hz, to be compared with 80 Hz of real Bhabha events at the same R. However, 30 Hz is clearly a very conservative limit, since (fig. 12 *ibidem*) most of the particles reach the endcap with both small radii and small momenta. As an example, a charged particle generated at the quadrupole and passing through the 'hottest wire' of the chamber (see definition in the text below), reaches the endcap at $R = 45\,\mathrm{cm}$. This corresponds to $\vartheta = 12.7^\circ$, and a minimum p of $70\,\mathrm{MeV}/c$ (for $p_\perp^{\mathrm{min}} = 15\,\mathrm{MeV}/c$).

Rounding up this figure, we define '1 KLOE year' as $100\,\mu$C/cm, the Bhabha dose accumulated on one cm of wire during one year of running at the maximum DAΦNE luminosity at this very extreme of drift chamber volume.

This is clearly still very pessimistic, since for example, due to the violent dependence of the Bhabha cross section on ϑ, $Q_{1\,\mathrm{year}}$=62$\,\mu$b on 1 cm of wire belonging to the second layer (30.5 cm$\leqslant R \leqslant$32.5 cm) at $|z| = 142$ cm, or $Q_{1\,\mathrm{year}}$=65$\,\mu$b on 1 cm of wire belonging to the first layer, but at $|z| = 132$ cm.

2. Test Setup

One operating parameter that is affected by the ageing of the wires is the gain of the cell. The lowering of the gas gain is due to the lowering of the electric field in the cell, which is in turn due to the accumulation of positive ions on the cathode (field) wires. The ion build up at the cathodes occurs in the presence of an insulating layer on the field wires which prevents the ions from leaving the cathodes. This insulating layer may develop after some time of operation and then continue to grow with time, thus worsening the performance of the device. The effect of such a deposit on the field wires can be seen observing the wires at the microscope, as they appear after a long exposure to radiation.

In fig. 1 a comparison between a new and an aged wire is shown; the solid deposits on the aged wire are most likely due to the polymerization of some molecules of the isobutane used as quencher in our gas mix, or some other pollutant that may be present in the gas and eventually deposit on the field wires. The gain stability of the device when illuminated with a constant source of ionising radiation, can be monitored by measuring the current drawn as a function of time.

2.1 The test tube

The test tube consisted of a $3 \times 3\,\mathrm{cm}^2$ square cell, with the sense wire in the centre and the field wires around. The two field to sense wire ratios $\mathcal{R}_{\mathrm{fs}}$=2 and 3 have been studied. The electrostatic configuration of the cell lattice of the final drift chamber was simulated by the layer of guard wires surrounding the field wires.

The wires were strung between two aluminum end plates carrying the pins, which were held together, 24 cm apart, by an aluminum cylinder providing mechanical rigidity and gas tightness.

The layout of the endplates is shown in fig. 2. The HV and readout electronics were placed at opposite ends.

Most of the runs were taken illuminating the cell, as it is shown in fig. 3, with the X-ray beam collinear with the wires. A kapton window with a diameter of 1 cm let the beam enter the cell undisturbed. Other two facing windows were cut on the aluminum cylinder surface, to allow irradiation perpendicular to the wires.

The choice of the voltages on the wires was guided by the criterion to have in the tube the same charge linear density as in previously studied prototypes with similar geometry and $\mathcal{R}_{\mathrm{fs}}$, both on the sense and on the field wires.

The gas gain depends not only on a possible ageing effect, but also on temperature, pressure and gas composition. To cancel out these effects, at least to first order, we normalized the current variations in the test tube to the ones from another tube. This monitor tube consisted of a small Plexiglas cylindrical tube containing an aluminized mylar straw-tube counter. The monitor tube preceded the test tube in a daisy-chain gas connection, so that an identical gas mixture was flowing in both of them.

An outline of the setup is shown in fig. 3. From left to right there are the X-ray tube with the beam collimator, the test prototype (hereafter also called prototype 0.4), and the monitor tube, which was made to draw some current [(2)] with a small β source placed upon it. The X-ray tube had a tungsten filament and adjustable operating voltage and current. We ran it stably at HV=25 kV, I=4 mA.

Power supply to the sense wires of both tubes was provided by a 2 channel high voltage module (CAEN N 471 A), which also read the current with a resolution of 1 nA. The guard wires of prototype 0.4 were powered by another module. Data acquisition was `CAMAC` based and was started every minute by a scaler. The quantities written on disk were the event date and time, the current drawn by the two tubes, and the temperature.

3. Experimental results

We have taken data in a five weeks period starting in March 1995, with four different configurations. For each of the two cell geometries (3:1 and 2:1) we tested two different wires: pure aluminum (Al) and aluminum with a silver coating (Al-Ag).

During the first two runs, one with a 3:1 Al-Ag wire and the following with a 2:1 Al-Ag wire, we have noticed a very fast and significant decrease in the cell gain, which reflected in a decrease in the observed current drawn by prototype 0.4, as shown in fig. 4. The same effect was not observed in the monitor tube, but was too big to be due to a real ageing of the wires. We attribute this effect to some kind of *gas ageing*, as the current (gain) went back to its starting value after we changed more than 4-5 gas volumes in prototype 0.4, while the X-ray source was turned off. This also can be seen in fig. 4.

(2) Typically a factor $\simeq 10$ less than in prototype 0.4, to avoid ageing in the monitor tube.

Since the gas was flowing at the rather slow rate of 0.5 l/h (the volume of the cylinder is approximately 1.2 l), we thought that the gas could somehow get poisoned by the ionising radiation as it circulated in the prototype. The rate of poisoning could be very fast, and in fact faster than that with which new gas was input in the cell.

To verify this we have changed the gas flow rate and noticed that indeed the current changed very rapidly, increasing with the flow rate and eventually reaching a plateau value; this is shown in fig. 5.

We have also irradiated the prototype with zero gas flow (closed bottle). The tube current rapidly decreased to zero, indicating a complete gas poisoning. After exchanging 4-5 gas volumes without X-rays, the current was back to its initial value, showing a full recovering of the cell.

A further evidence of this was obtained when we run with the X-ray beam transverse to the wires direction. The current drawn by the tube was about 1/8th of that drawn with the beam parallel to the wires, correponding to the expected ratio of illuminated volumes of $3\,\mathrm{cm}/24\,\mathrm{cm}=1/8$. The flow at which the plateau current is reached was however lower, ~ 1.5 l/h.

To avoid this *flow* or *gas damage* effect in trying to extract the *wire ageing*, we took all the subsequent runs at a flow rate for which the current was close to its plateau value. For the Al-Ag configurations, a flow rate of $\simeq 2.5$ l/h was chosen, while in the last run of our beam time, corresponding to the Al 2:1 configuration, we could flux at $\simeq 3.5$ l/h, without worrying about finishing our gas supplies. For lack of beam time we did not repeat the run for the configuration 3:1-Al wire; an upper value for its ageing, however, is given by that of the 2:1-Al configuration.

In figs. 6–8 the current is shown as a function of integrated charge on the wire in mC/cm; referring to the definition in sec. 1.1, 1 mC/cm is equivalent to 10 KLOE years. In fig. 8 the peaks are due to some environmental effect, since they occurred exactly at the same time for three consecutive days, and are not caused by the prototype. The results are summarized in table 1. The lower ageing of the Al 2:1 configuration may be in part due to the higher flow rate used.

Configuration	$\frac{Q}{L}$ [mC/cm]	$\frac{\Delta I}{I}$ [%]
Al-Ag 2:1	2.3	4
Al-Ag 3:1	2.7	5
Al 2:1	3.1	$\simeq 0$

Tab. 1: *Summary of ageing results.*

No dark current has ever been observed: the current in prototype 0.4 went to zero immediately after switching off the X-ray source, even after long radiation exposures. Finally, we inspected visually the W sense wire, without noticing any modification on its surface; no clear evidence of wire ageing has been observed on the field wires either, in the high gas flow environment.

4. Conclusions

We can conclude from this analysis that the ageing of both kind of wires, in any of the two proposed KLOE cell configurations, is negligible.

We have observed an effect of *gas damage* that varies with the gas flow rate. The values of flow rate at which these effects take place are however very low, in fact so low that they will probably never emerge in the KLOE final chamber,[(3)] and then disappears for sufficiently high flow rates. Nevertheless the (at least theoretical) occurrence of such effects will have to be taken into account to choose the flow rate of the final chamber.

As a final remark, we stress that our equipment was by no means optimised for what the control of impurities in the gas is concerned. We used PVC gas tubes rather than the steel ones that will probably be used in the final system. Since it is well known [6] that the presence of gas pollutants deteriorates the ageing performance of gaseous detectors, our results should represent a conservative limit.

ACKNOWLEDGEMENTS

We wish to thank Dr. Roberto Felici for his kind hospitality in the laboratory at Istituto di Struttura della Materia of CNR, and for use of the X-ray gun. We also thank E. Iacuessa for constructing the test tube.

REFERENCES

1. S. Guiducci, *Background in the KLOE IR due to Touscheck Scattering*, DAΦNE technical note IR-5 1994.
2. E. Gero, *Beam-gas Background Calculations for* DAΦNE, KLOE note n. 102 (March 1994).
3. E. Drago, A. Smilzo, *Energy release by small angle Bhabha events in EMC endcaps: 2*, KLOE note n. 118 (June 1994).
4. G. Bencivenni, A. Calcaterra, M. Carletti, R. de Sangro, G. Felici, G. Finocchiaro, M. Piccolo, P. Santantonio, *The Prototype 0 of the KLOE Drift Chamber*, KLOE note n. 79 (December 1993).

(3) We integrated typically 1.2 mC/cm in one day, corresponding (sec. 1.1) to 6 months of Bhabha irradiation in one hour. Since in the same period two gas volumes are exchanged at the quoted flow rate of 2.5 l/h, this would correspond to 1 gas change in three months of operation in the KLOE drift chamber.

5. H. Fischle, J. Heintze and B. Schmidt, *NIM* **A301**, 202 (1991).
6. J. Va'vra, *NIM* **A552**, 547 (1986).

FIGURE CAPTIONS

1. Picture of the field wires with 250X magnification.
2. Layout of one endplate of prototype 0.4.
3. Artist's view of the experimental setup.
4. Current vs. time in prototype 0.4 with Al-Ag wires and $\mathcal{R}_{\mathrm{fs}}$=2, ϕ=0.5 l/h.
5. Current drawn by the prototype vs. gas flow rate.
6. Current vs. integrated charge per unit length. $\mathcal{R}_{\mathrm{fs}}$=2, Al-Ag wires, ϕ=2.5 l/h.
7. Current vs. integrated charge per unit length. $\mathcal{R}_{\mathrm{fs}}$=3, Al-Ag wires, ϕ=2.5 l/h.
8. Current vs. integrated charge per unit length. $\mathcal{R}_{\mathrm{fs}}$=2, Al wires, ϕ=3.5 l/h.

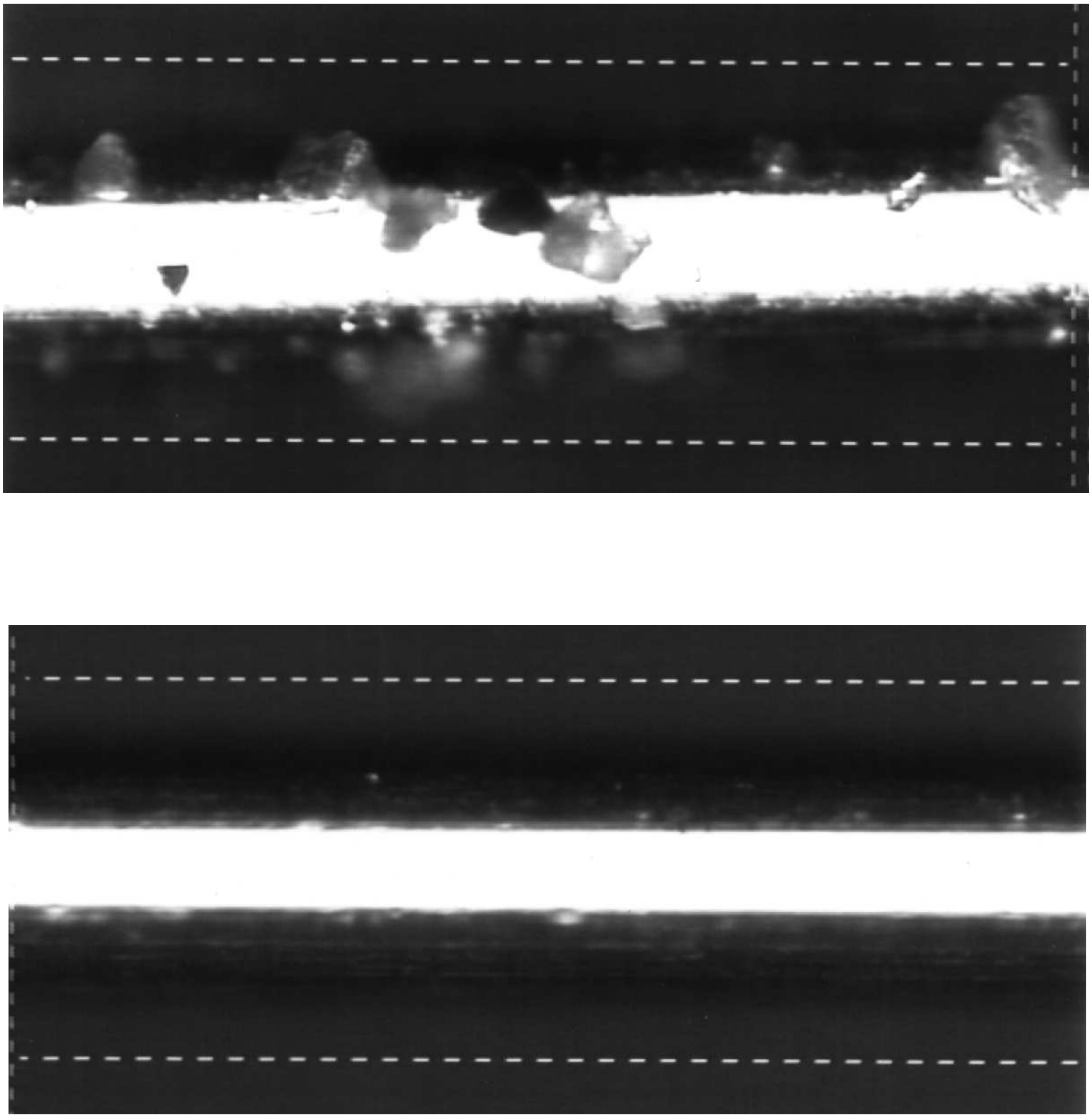

Fig. 1: *Photograph of the field wires with 200X magnification; (a) field wire on the same side of the photon source and (b) one on the opposite side. The photo in (a) refers to a portion of wire irradiated at low gas flow (see text).*

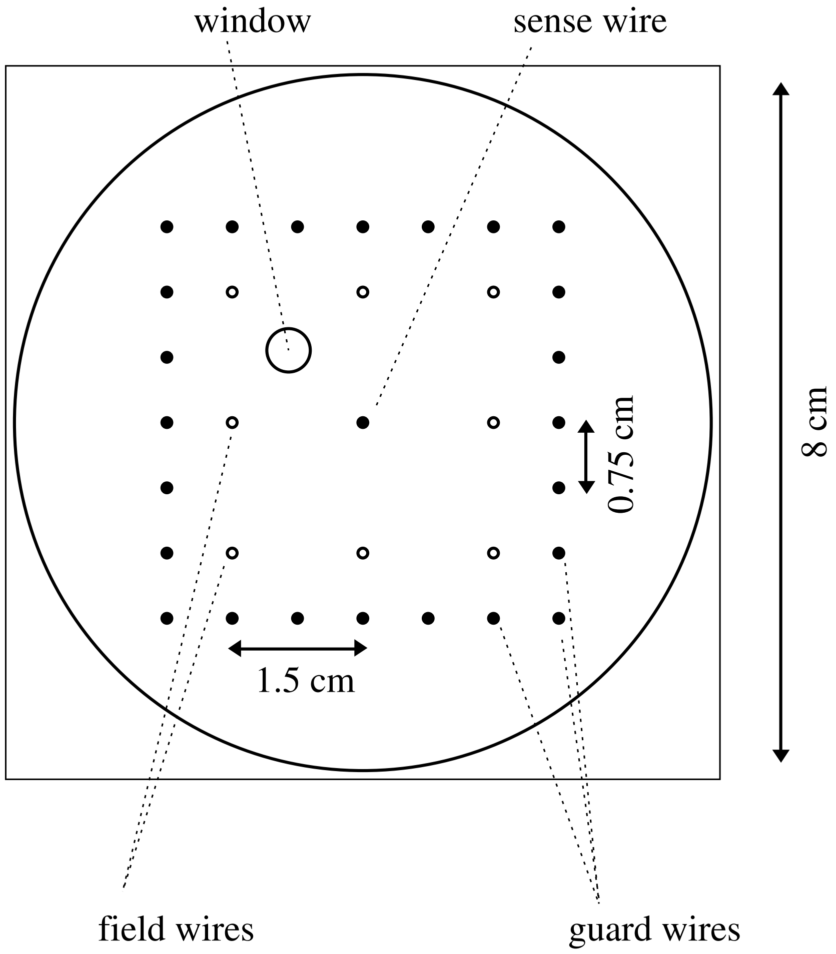

Fig. 2: *Layout of one endplate of prototype 0.4.*

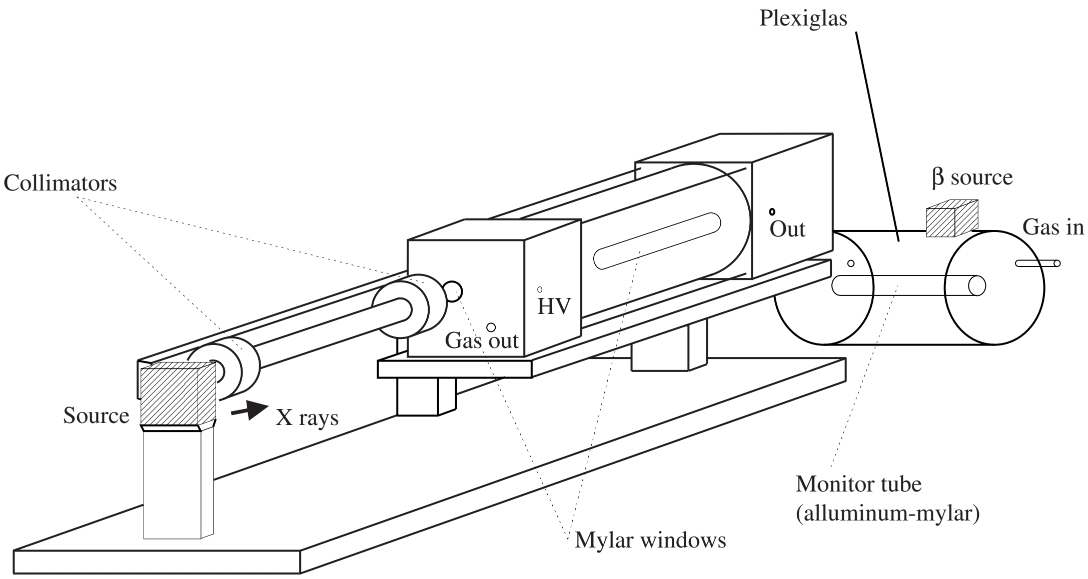

Fig. 3: *Artist's view of the experimental setup.*

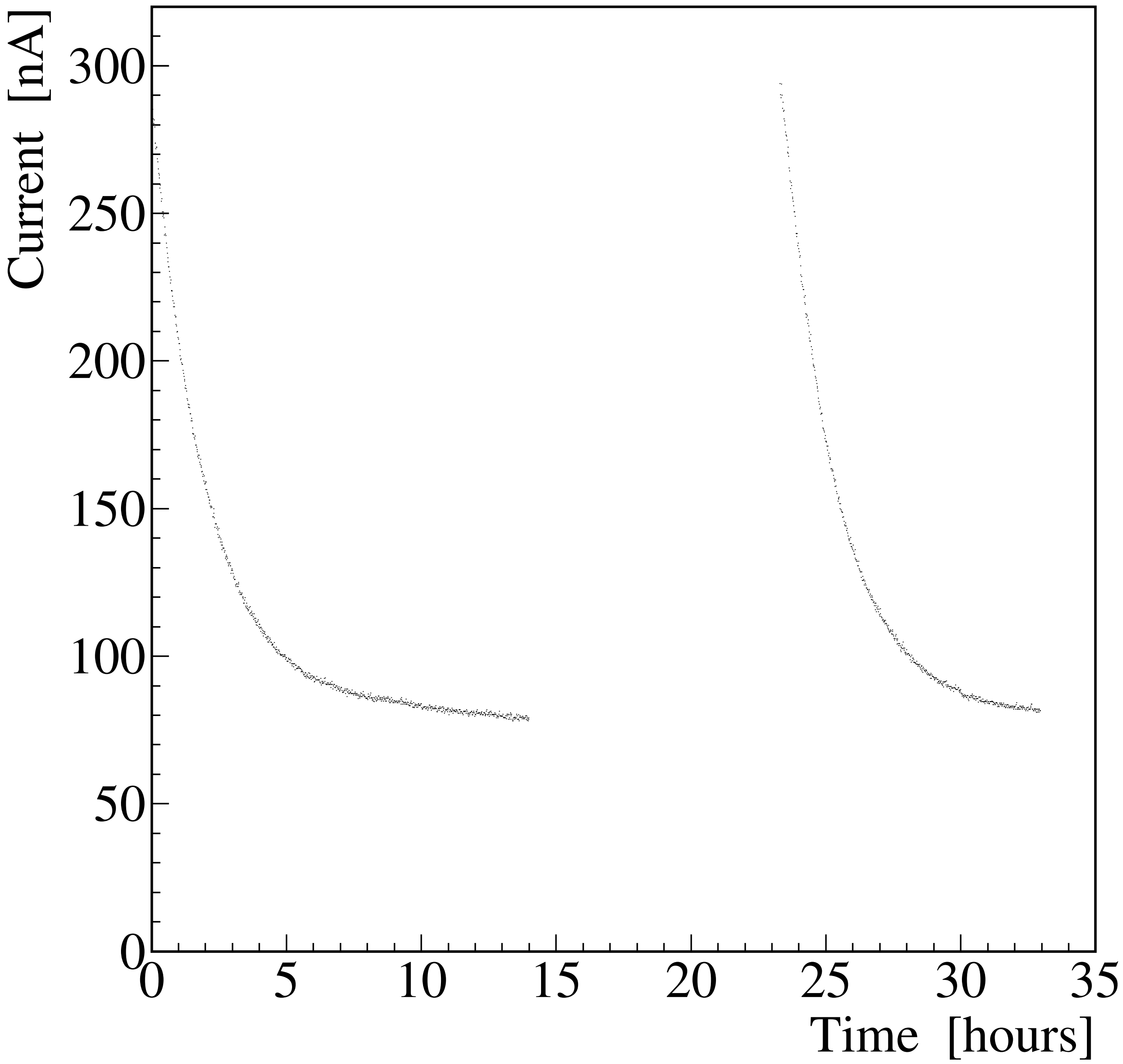

Fig. 4: *Current vs. time in prototype 0.4 with Al-Ag wires and $\mathcal{R}_{\rm fs}$=2. The rapid decrease of the current is due to the low gas flow rate (0.5 l/h).*

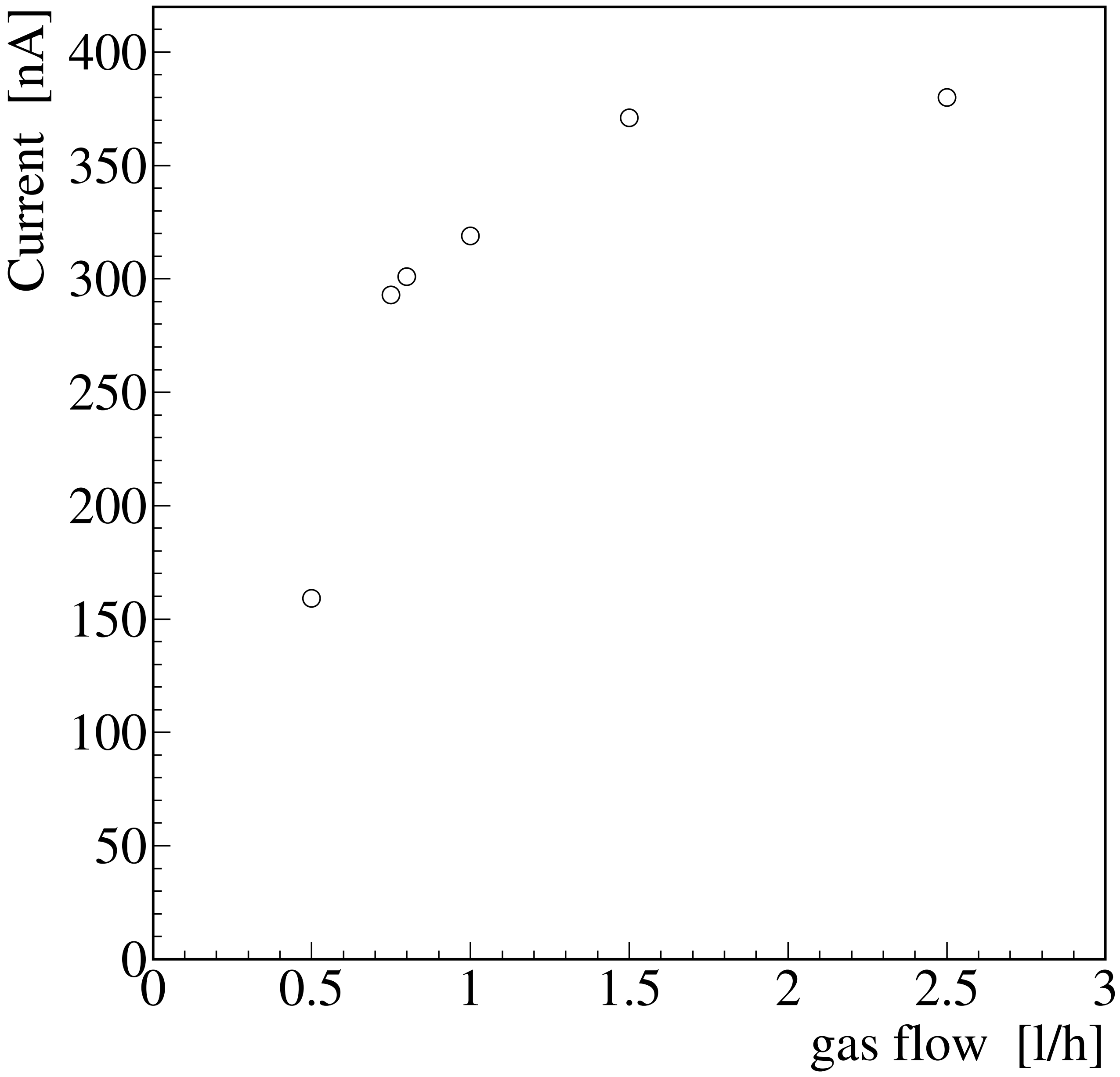

Fig. 5: *Current drawn by the prototype vs. gas flow rate.*

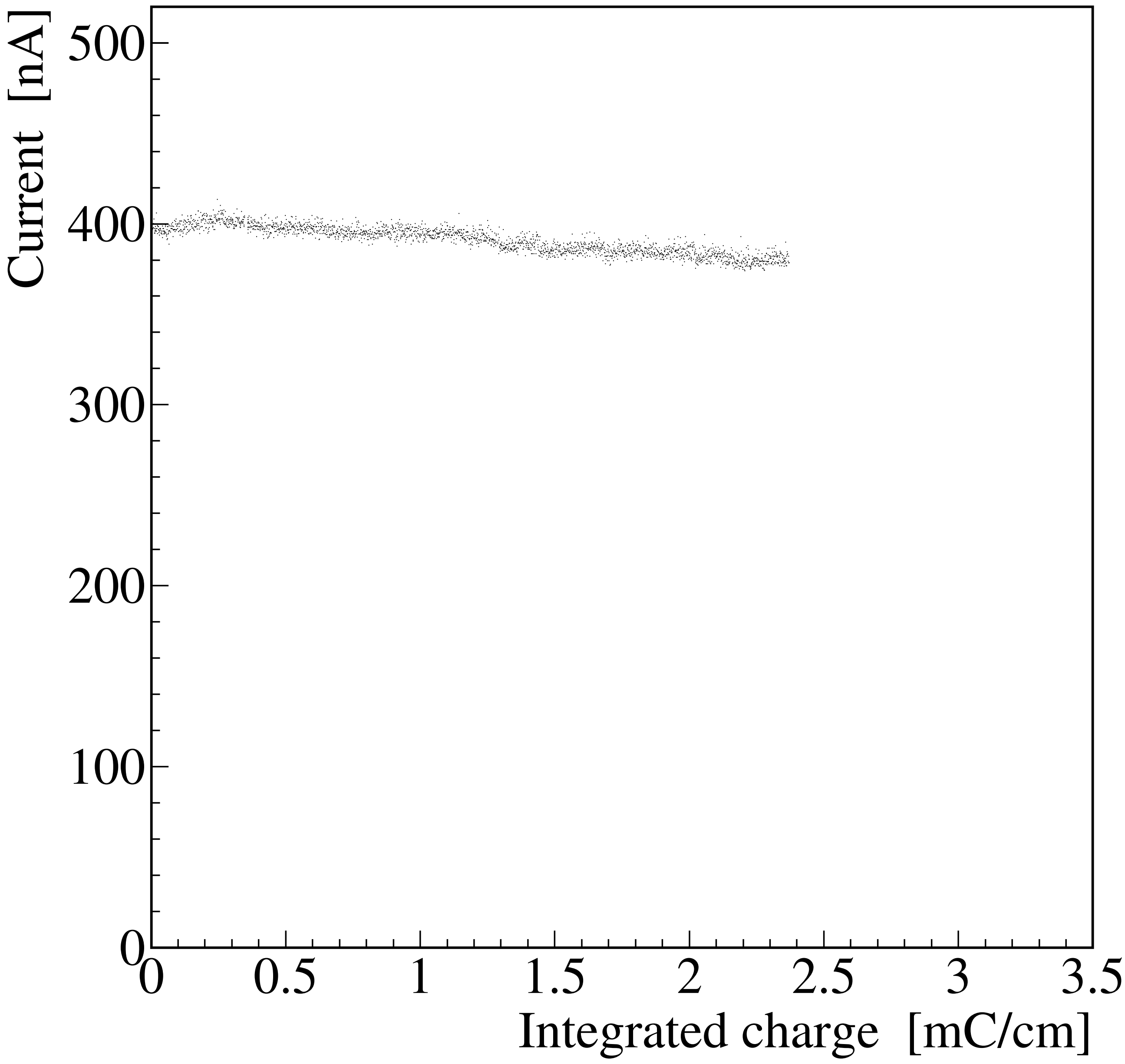

Fig. 6: *Current vs. integrated charge per unit length.* $\mathcal{R}_{\rm fs}$*=2, Al-Ag wires,* ϕ*=2.5 l/h.*

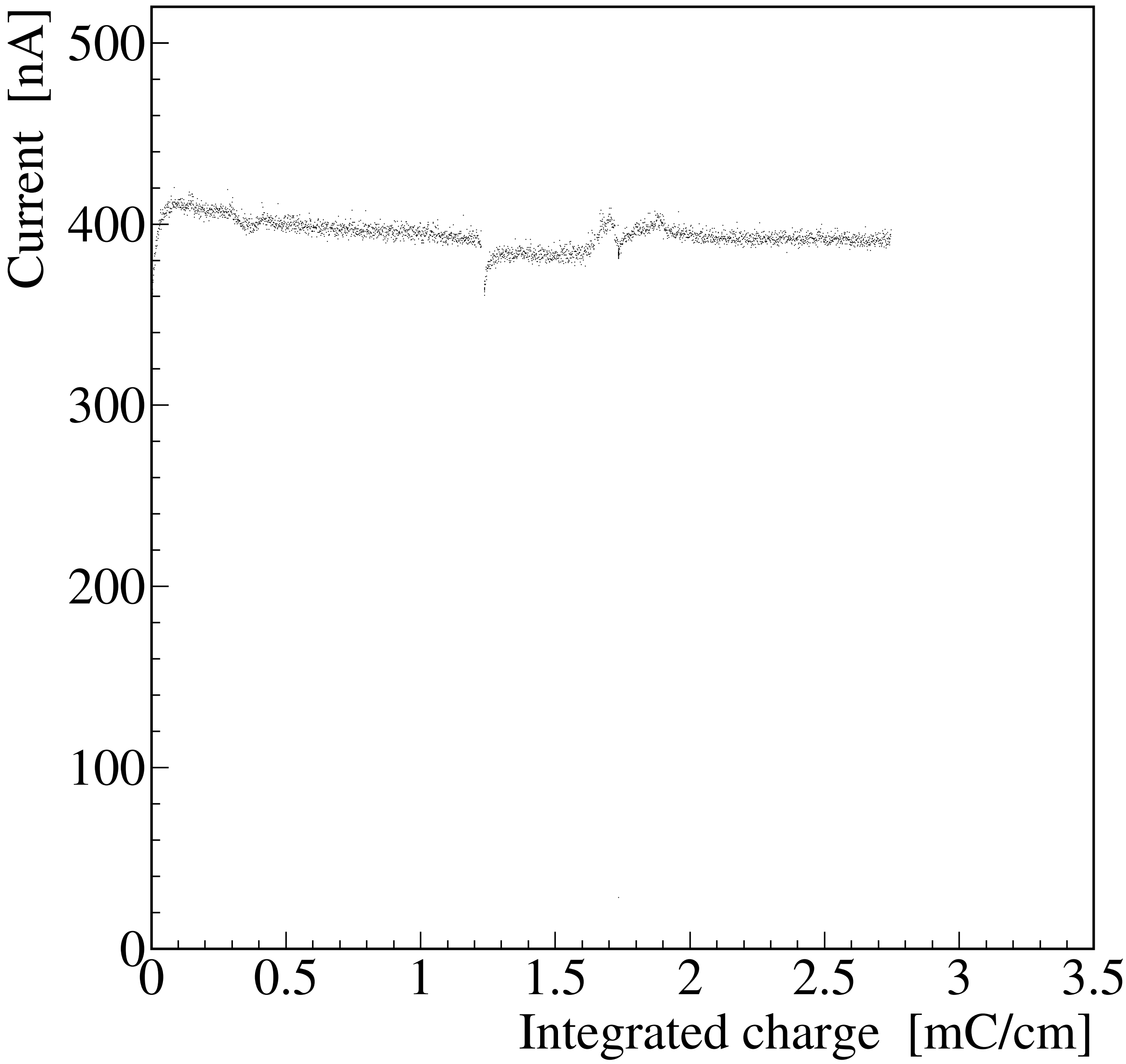

Fig. 7: *Current vs. integrated charge per unit length.* $\mathcal{R}_{\mathrm{fs}}$*=3, Al-Ag wires,* ϕ*=2.5 l/h.*

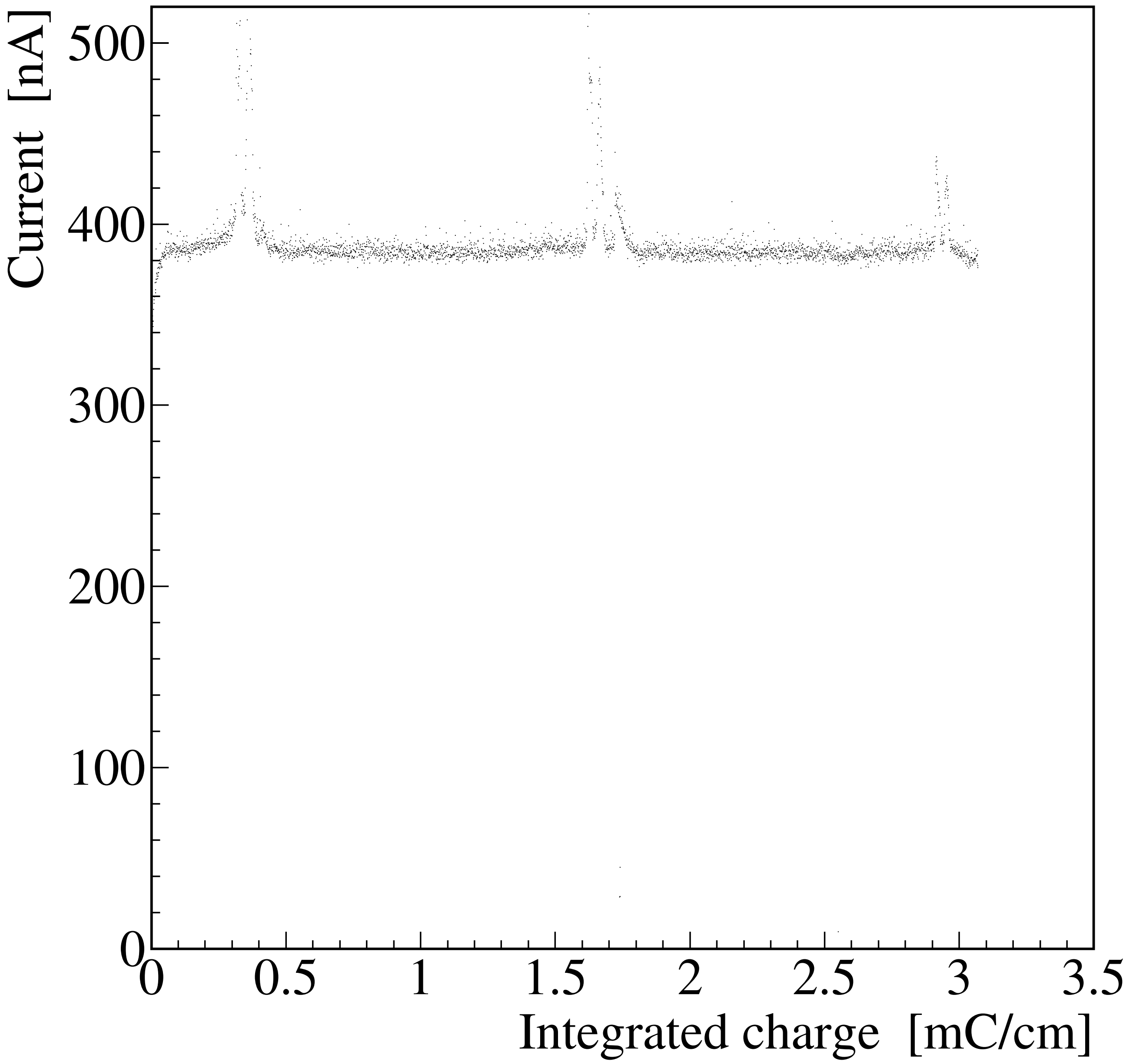

Fig. 8: *Current vs. integrated charge per unit length. $\mathcal{R}_{\mathrm{fs}}$=2, Al wires, ϕ=3.5 l/h. The peaks on top of the flat curve (occurring at 16:45 of three consecutive days) are* not *correlated with prototype 0.4.*